Journal Pre-proofs

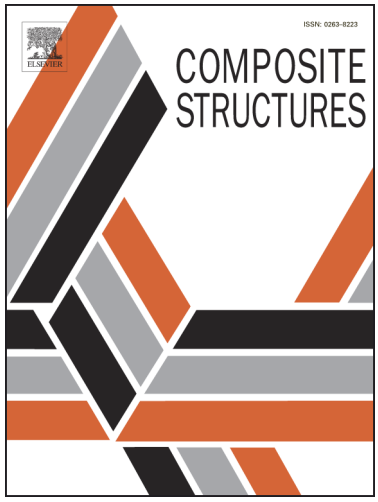

On torsion of nonlocal Lam strain gradient FG elastic beams

R. Barretta, S. Ali Faghidian, F. Marotti de Sciarra, R. Penna, F.P. Pinnola

PII: S0263-8223(19)33283-0
DOI: https://doi.org/10.1016/j.compstruct.2019.111550
Reference: COST 111550

To appear in: *Composite Structures*

Received Date: 30 August 2019
Revised Date: 6 October 2019
Accepted Date: 9 October 2019

Please cite this article as: Barretta, R., Ali Faghidian, S., de Sciarra, F.M., Penna, R., Pinnola, F.P., On torsion of nonlocal Lam strain gradient FG elastic beams, *Composite Structures* (2019), doi: https://doi.org/10.1016/j.compstruct.2019.111550

On torsion of nonlocal Lam strain gradient FG elastic beams

R. Barretta [a], S. Ali Faghidian [b], F. Marotti de Sciarra [a], R. Penna [c], F. P. Pinnola [a]

[a] *Department of Structures for Engineering and Architecture, University of Naples Federico II, via Claudio 21, 80125 Naples, Italy – e-mails: rabarret@unina.it - marotti@unina.it - francescopaolo.pinnola@*unina.it

[b] *Department of Mechanical Engineering, Science and Research Branch, Islamic Azad University, Tehran, Iran – e-mail: faghidian@gmail.com*

[c] *Department of Civil Engineering, University of Salerno, via Giovanni Paolo II, 132, 84084 Fisciano (Sa), Italy – e-mail: rpenna@unisa.it*

Abstract

The nonlocal strain gradient theory of elasticity is the focus of numerous studies in literature. Eringen's nonlocal integral convolution and Lam's strain gradient model are unified by a variational methodology which leads to well-posed structural problems of technical interest. The proposed nonlocal Lam strain gradient approach is presented for functionally graded (FG) beams under torsion. Static and dynamic responses are shown to be significantly affected by size effects that are assessed in terms of nonlocal and gradient length parameters. Analytical elastic rotations and natural frequencies are established by making recourse to a simple solution procedure which is based on equivalence between integral convolutions and differential equations supplemented with variationally consistent (but non-standard) nonlocal boundary conditions. Effects of Eringen's nonlocal parameter and stretch and rotation gradient parameters on the torsional behavior of FG nano-beams are examined and compared with outcomes in literature. The illustrated methodology is able to efficiently model both stiffening and softening torsional responses of modern composite nano-structures by suitably tuning the small-scale parameters.

Keywords

Torsion; FG nano-beams; Lam strain gradient elasticity; nonlocal integral elasticity; modified nonlocal strain gradient elasticity; size effects; analytical modelling; NEMS.

1. Introduction

Recent advances in nano-engineering have led to rapid development of smaller and smaller devices in Nanotechnology. Nano-Electro-Mechanical Systems (NEMS) have indeed found a variety of applications in modern nano-systems such as, scanning mirror resonators [1], torsional accelerometer [2], torsional resonator [3], torsional nano-varactor [4], torsional magnetometer [5] and piezoelectric actuators [6]. Mechanical responses of torsional elements of nanoscopic structures should be modelled to achieve optimum design and functionality. However, the well-established approaches of local continuum mechanics are not able to capture size-effects at nano-scales. Nowadays, a variety of higher-order continuum theories, comprising scale parameters, are exploited to model the size-dependency of nano-structures. Characterization and assessment of mechanical responses of nano-structures have attracted enormous attention in the current literature, see e.g. [7-29] and review contributions [30, 31].

In the nonlocal theory of elasticity, nonlocal fields are defined by integral convolutions involving elastic source fields and appropriately selected averaging kernels. Based on the choice of source fields, two basic nonlocal formulations of strain- and stress-driven nonlocal elasticity are considered in literature. The resulted integro-differential equations of the strain-driven Eringen nonlocal integral theory [32] may be replaced with equivalent differential conditions on unbounded domains under the condition of vanishing stress field at infinity. Eringen nonlocal integral model leads to ill-posed structural problems of applicative interest, which are defined in bounded domains, due to incompatibility between constitutive and equilibrium requirements [33-35]. The stress-driven nonlocal formulation, recently conceived in [36], leads instead to well-posed structural problems in nano-engineering. The consistent pure and two-phase stress-driven nonlocal elasticity were successfully exploited to analyze size-dependent elastostatic [37-44] and elastodynamic [45-49] responses of nano-structures.

The strain gradient elasticity theory amounts to a gradient-type material reactive to strain gradients, and consequently, the material behavior of a continuum not only depends on the strain field but also on the gradients of the strain field. The general strain gradient elastic theory was conceived by Mindlin [50] to examine size-dependent responses of elastic materials with micro-structural effects. Advantageously, simplified and modified strain gradient models of elasticity were proposed by Aifantis [51] and Lam et al. [52]. The strain gradient elasticity can be employed to analyze nano-continuu problems, although it is well-known to merely exhibit stiffening structural behaviors.

The nonlocal strain gradient theory of elasticity was introduced by Aifantis [53, 54] as a unified gradient elasticity theory demonstrating the effects of both strain and stress gradients on the constitutive response of elastic materials. The higher-order nonlocal strain gradient theory was then established by Lim et al. [55] by combining the Eringen nonlocal theory and the simplified strain gradient formulation by making recourse to a thermodynamic approach. In nonlocal strain gradient theory, the elasticity form of the stationary Reissner variational principle was proposed [56] and exploited to establish the corresponding beam model [57]. The second-order integro-differential elasticity theory within the thermodynamic framework was also established in [58] introducing the nonlocal effects of higher-order strain gradients. While higher-order boundary conditions associated with the nonlocal strain gradient integral law are not required to be introduced in the analysis of rapidly vanishing fields at infinity, appropriate constitutive boundary conditions should be adopted to close nonlocal strain gradient problems in bounded domains. This objective has been achieved in [59] by detecting appropriate higher-order boundary conditions of constitutive type generating thus the consistent modified nonlocal strain gradient formulation of elasticity. The methodology has been recently utilized to effectively assess size-dependent elasto-static and -dynamic behaviors of structures for nano-engineering applications [60-62].

Structural elements of modern NEMS can often experience torsional deformations, and accordingly, a variety of nonlocal models have been exploited to examine scale phenomena. Instances are as follows: Eringen nonlocal differential model [63-66], Eringen nonlocal viscoelastic model [67, 68], enhanced Eringen nonlocal model [69], strain gradient theory [70-72], stress-driven nonlocal theory [73], mixture stress-driven integral model [74], mixture strain-driven integral model [75] and nonlocal strain gradient theories of elasticity [76, 77]. In the present study, the torsion behavior of functionally graded (FG) elastic nano-beams is analyzed in the novel framework of nonlocal Lam strain gradient elasticity. The proposed formulation can efficiently capture effects of nonlocality of the nano-structure stretch and rotation gradients. Easto-static and -dynamic torsional responses of FG elastic beams are analytically investigated. The outcomes are then compared with the numerical results obtained by the modified nonlocal strain gradient theory. New benchmark examples for nonlocal strain gradient continuum mechanics are also detected that can be advantageously employed for design and optimization of torsional parts of new-generation NEMS.

2. Variational elasticity for nonlocal Lam strain gradient FG beams under torsion

Let us consider a straight elastic beam of length $L = b - a$, having an annular circular cross-section with inner and outer radii r_i and r_o occupying a domain Ξ, as schematically depicted in Fig. 1. The abscissa x is selected along the beam axis and the axes (y, z) represent cartesian components of the position vector $\mathbf{r}$ of a cross-sectional point with respect to the centroid. The FG nano-beam is considered to be made of two different elastically homogeneous materials with densities ρ_i, ρ_o and shear moduli G_i, G_o, respectively at the inner and outer surfaces. Thus, the effective material properties of the FG nano-beam continuously vary along the radial direction $\mathbf{r}$ in the beam cross-section plane.

Shear modulus and material density are therefore assumed to vary along the radial direction according to the general form

$$G = G(\mathbf{r}), \qquad \rho = \rho(\mathbf{r}) \tag{1}$$

To examine the size-dependent behaviour of FG elastic nano-beams with continuous radial variation of material properties, it is convenient to introduce the effective local elastic shear stiffness A_G and effective torsional stiffness J_G as

$$A_G = \iint_{\Xi} G(\mathbf{r})dA, \qquad J_G = \iint_{\Xi} G(\mathbf{r})(\mathbf{r}\cdot\mathbf{r})dA \tag{2}$$

with the dot into the integrals standing for inner product between vectors. Likewise, the effective mass polar moment of inertia J_ρ, to be employed in the elasto-dynamic torsional analysis of FG nano-beam, is introduced as

$$J_\rho = \iint_{\Xi} \rho(\mathbf{r})(\mathbf{r}\cdot\mathbf{r})dA \tag{3}$$

A detailed discussion on elastic properties of FG cross-sections in the torsion analysis is provided in Ref. [67].

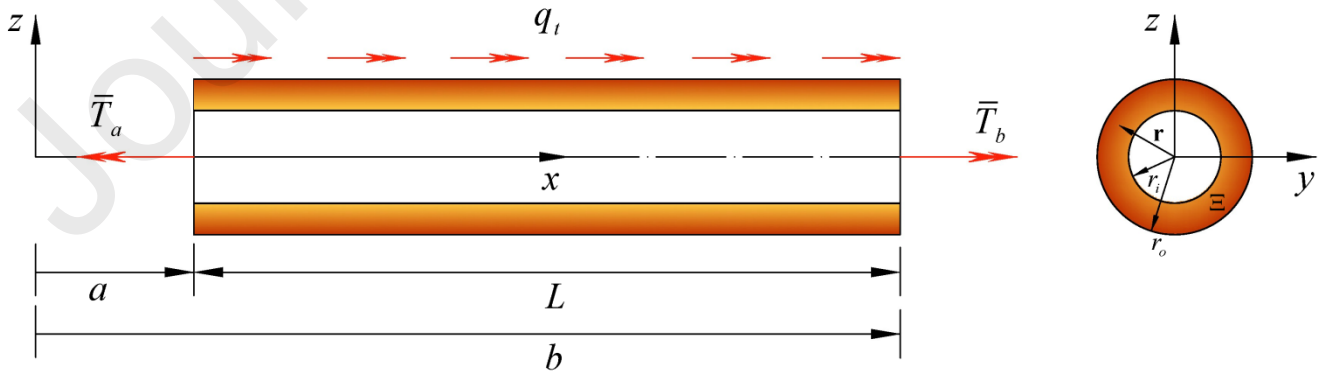

Fig. 1. Coordinate system and configuration of a FG beam under torsion

Cartesian components of the displacement field of the beam under torsion, up to an inessential additional rigid body motion, take the form

$$u_x = 0, \qquad u_y = -\varphi(x)z, \qquad u_z = \varphi(x)y \tag{4}$$

with $\varphi:[a,b]\mapsto\Re$ standing for torsional rotation.

The non-vanishing kinematically compatible shear strain field is accordingly provided by

$$\boldsymbol{\gamma} = \mathbf{R}\mathbf{r}\kappa(x,t) = \mathbf{R}\mathbf{r}\partial_x\varphi(x,t) \tag{5}$$

where $\kappa = \partial_x\varphi:[a,b]\mapsto\Re$ is the geometric torsional curvature along with the shear strain vector $\boldsymbol{\gamma}$, shear stress vector $\boldsymbol{\tau}$, position vector $\mathbf{r}$ and rotation tensor $\mathbf{R}$ expressed by

$$\boldsymbol{\gamma} = \begin{bmatrix} \gamma_{yx} \\ \gamma_{zx} \end{bmatrix}, \qquad \boldsymbol{\tau} = \begin{bmatrix} \tau_{yx} \\ \tau_{zx} \end{bmatrix}, \qquad \mathbf{r} = \begin{bmatrix} y \\ z \end{bmatrix}, \qquad \mathbf{R} = \begin{bmatrix} 0 & -1 \\ 1 & 0 \end{bmatrix} \tag{6}$$

The vector $\mathbf{R}\mathbf{r}$ provides the $\pi/2$ counterclockwise rotation of position vector $\mathbf{r}$.

The beam is assumed to be subjected to distributed torsional couples per unit-length $q_t:[a,b]\mapsto\Re$ and concentrated couples at the end cross-sections $\bar{T}_a$ and $\bar{T}_b$. Standardly, the differential and boundary conditions of equilibrium write as

$$\begin{aligned} &\partial_x T + q_t = J_\rho \partial_{tt}\varphi \\ &\left(T + \bar{T}_a\right)\delta\varphi\big|_{x=a} = \left(T - \bar{T}_b\right)\delta\varphi\big|_{x=b} = 0 \end{aligned} \tag{7}$$

where the twisting resultant moment is denoted by T and provided by

$$T = \iint_{\Xi} (\mathbf{R}\mathbf{r}) \times \boldsymbol{\tau} dA \tag{8}$$

The total potential energy U, consistent with modified strain gradient theory of Lam et al. [52], depends on the torsional curvature $\kappa \in C^2([a,b];\Re)$ and may be shown to be [70]

$$U(\kappa) := \frac{1}{2}\int_a^b \left(\left(J_G + 3A_G \ell_2^2\right)\kappa^2 + J_G \left(\frac{8}{15}\ell_1^2 + \frac{1}{4}\ell_2^2 \right)\left(\partial_x \kappa\right)^2 \right) dx \tag{9}$$

where ℓ_1 and ℓ_2 correspondingly designate the gradient characteristic parameters associated with the nano-structural stretch and rotation gradients. The effective local elastic shear stiffness A_G and effective torsional stiffness J_G are also given by Eq. (2).

Motivated by the milestone approach of Eringen [32], the nonlocal Lam strain gradient model of torsion problem can be formulated by including nonlocal integral convolution in Eq. (9). The total elastic strain energy of nonlocal Lam strain gradient FG nano-beams under torsion Π is

$$\Pi(\kappa) := \frac{1}{2}\int_a^b \left(\left(J_G + 3A_G \ell_2^2\right)\left(\psi_\lambda * \kappa\right)\kappa + J_G \left(\frac{8}{15}\ell_1^2 + \frac{1}{4}\ell_2^2 \right)\left(\psi_\lambda * \partial_x \kappa\right)\left(\partial_x \kappa\right) \right) dx \tag{10}$$

where the integral convolution of a scalar field f with a smoothing kernel ψ_λ is defined by

$$\left(\psi_\lambda * f\right)(x) := \int_a^b \psi_\lambda (x - \bar{x}) f(\bar{x}) d\bar{x} \tag{11}$$

The smoothing kernel ψ_λ is well-established to fulfil the positivity and parity, symmetry, normalization and limit impulsivity properties [33-35].

The twisting moment in the nonlocal Lam strain gradient model $T \in C^1\left([a,b];\Re\right)$ is established via a mathematically well-posed variational constitutive condition as follows

$$\langle T, \delta\kappa \rangle := \int_a^b T(x)\delta\kappa(x) dx = \langle d\Pi(\kappa), \delta\kappa \rangle \tag{12}$$

for any virtual torsional curvature field $\delta\kappa \in C_0^1\left([a,b];\Re\right)$ having compact support in $[a,b]$.

The directional derivative of the elastic strain energy along a virtual torsional curvature can be determined via introducing the expression of Π as Eq. (10) based on integration by parts

$$\begin{aligned}\left\langle d\Pi(\kappa),\delta\kappa\right\rangle &= \int_a^b \left(\left(J_G + 3A_G\ell_2^2\right)\left(\psi_\lambda * \kappa\right)\delta\kappa + J_G\left(\frac{8}{15}\ell_1^2+\frac{1}{4}\ell_2^2\right)\left(\psi_\lambda * \partial_x\kappa\right)\partial_x\left(\delta\kappa\right)\right)dx \\ &= \int_a^b \left(\left(J_G + 3A_G\ell_2^2\right)\left(\psi_\lambda * \kappa\right) - J_G\left(\frac{8}{15}\ell_1^2+\frac{1}{4}\ell_2^2\right)\partial_x\left(\psi_\lambda * \partial_x\kappa\right)\right)\delta\kappa dx \\ &+ J_G\left(\frac{8}{15}\ell_1^2+\frac{1}{4}\ell_2^2\right)\left(\left(\psi_\lambda * \partial_x\kappa\right)\delta\kappa\big|_{x=b} - \left(\psi_\lambda * \partial_x\kappa\right)\delta\kappa\big|_{x=a}\right)\end{aligned} \tag{13}$$

The test fields $\delta\kappa \in C_0^1\left(\left[a,b\right];\Re\right)$ in the variational condition Eq. (12) have compact supports, so that $\delta\kappa\big|_{x=a} = \delta\kappa\big|_{x=b} = 0$, and thus the boundary terms in Eq. (13) are disappearing.

A standard localization procedure provides the nonlocal strain gradient twisting moment T in terms of the torsional curvature field κ while imposing the variational condition Eq. (12)

$$T\left(x\right) = \left(J_G + 3A_G\ell_2^2\right)\left(\psi_\lambda * \kappa\right)\left(x\right) - J_G\left(\frac{8}{15}\ell_1^2+\frac{1}{4}\ell_2^2\right)\partial_x\left(\psi_\lambda * \partial_x\kappa\right)\left(x\right) \tag{14}$$

The equivalent differential constitutive problem with the corresponding constitutive boundary conditions associated with the nonlocal Lam strain gradient model (NLSG) are determined following the mathematically well-posed approach by Barretta and Marotti de Sciarra [59]. The smoothing kernel ψ_λ in the nonlocal integral convolution Eq. (14) is assumed to be the Helmholtz bi-exponential function considered in Eringen nonlocal theory

$$\psi_\lambda\left(x\right) := \frac{1}{2L_c}\exp\left(-\frac{\left|x\right|}{L_c}\right) \tag{15}$$

where the nonlocal characteristic length $L_c = \lambda L$ describes long-range interactions.

Proposition. *The nonlocal strain gradient constitutive law Eq*. (14), *endowed with the Helmholtz bi-exponential kernel Eq*. (15), *is equivalent to the differential constitutive law*

$$T\left(x\right) - L_c^2\partial_{xx}T\left(x\right) = \left(J_G + 3A_G\ell_2^2\right)\kappa\left(x\right) - J_G\left(\frac{8}{15}\ell_1^2+\frac{1}{4}\ell_2^2\right)\partial_{xx}\kappa\left(x\right) \tag{16}$$

equipped with the constitutive boundary conditions (*CBC*)

$$\begin{aligned}&\partial_x T\left(a\right)-\frac{1}{L_c}T\left(a\right)=\frac{1}{L_c^2}J_G\left(\frac{8}{15}\ell_1^2+\frac{1}{4}\ell_2^2\right)\partial_x\kappa\left(a\right)\\&\partial_x T\left(b\right)+\frac{1}{L_c}T\left(b\right)=\frac{1}{L_c^2}J_G\left(\frac{8}{15}\ell_1^2+\frac{1}{4}\ell_2^2\right)\partial_x\kappa\left(b\right)\end{aligned}\tag{17}$$

The introduced non-standard boundary conditions Eq. (17) are of constitutive type, naturally associated with the nonlocal Lam strain gradient law Eq. (16) for twisted FG elastic nano-beams. Noteworthy, the constitutive boundary conditions do not contradict equilibrium requirements and thus result in mathematically well-posed size-dependent problems.

As the nonlocal characteristic length tends to zero, the Lam strain gradient model of straight beams under torsion can be recovered as a particular limiting case of the nonlocal Lam strain gradient law. Due to the limit impulsivity property of kernel ψ_λ, nonlocal strain gradient constitutive law Eq. (14) can be simplified to the Lam strain gradient differential equation

$$T\left(x\right)=\left(J_G+3A_G\ell_2^2\right)\kappa\left(x\right)-J_G\left(\frac{8}{15}\ell_1^2+\frac{1}{4}\ell_2^2\right)\partial_{xx}\kappa\left(x\right)\tag{18}$$

equipped with higher-order boundary conditions determined via simplifying NLSG CBC Eq. (17) on beam ends $\partial\left[a,b\right]$ as

$$\begin{aligned}&J_G\left(\frac{8}{15}\ell_1^2+\frac{1}{4}\ell_2^2\right)\partial_x\kappa\left(a\right)=0\\&J_G\left(\frac{8}{15}\ell_1^2+\frac{1}{4}\ell_2^2\right)\partial_x\kappa\left(b\right)=0\end{aligned}\tag{19}$$

The gradient constitutive law Eq. (18) and the associated non-standard boundary conditions Eq. (19) can be also detected by a formal application of Hamilton's principle [70].

Nonlocal strain gradient model suffers from prescribing un-motivated higher-order boundary conditions of strain gradient theory. On the contrary, the consistent form of constitutive boundary conditions suitably associated with the nonlocal strain gradient constitutive law is recently introduced in the framework of modified nonlocal strain gradient model [59].

Modified nonlocal strain gradient model (MNSG) leads to well-posed problems, and thus, it is selected here for comparison sake. The formulation of MNSG is briefly recalled as follows.

MNSG model of FG elastic beam under torsion is formulated by expressing the twisting resultant moment T in terms of two integral convolutions guided by elastic torsional curvature κ and by its gradient along the beam axis $\partial_x \kappa$ as

$$T(x) = J_G(\psi_\lambda * \kappa)(x) - J_G \ell_s^2 \partial_x (\psi_\lambda * \partial_x \kappa)(x) \tag{20}$$

where gradient characteristic length ℓ_s is introduced in the MNSG to make dimensionally homogeneous the convolutions in Eq. (20). Following the seminal contribution by Barretta and Marotti de Sciarra [59], it may be shown that the nonlocal strain gradient constitutive law Eq. (20) equipped with the Helmholtz bi-exponential kernel Eq. (15) is equivalent to the differential constitutive relation

$$T(x) - L_c^2 \partial_{xx} T(x) = J_G \kappa(x) - J_G \ell_s^2 \partial_{xx} \kappa(x) \tag{21}$$

equipped with the constitutive boundary conditions at the beam ends $\partial[a,b]$

$$\begin{aligned} &\partial_x T(a) - \frac{1}{L_c} T(a) = \frac{\ell_s^2}{L_c^2} J_G \partial_x \kappa(a) \\ &\partial_x T(b) + \frac{1}{L_c} T(b) = \frac{\ell_s^2}{L_c^2} J_G \partial_x \kappa(b) \end{aligned} \tag{22}$$

Notwithstanding that the constitutive boundary conditions are naturally associated with the nonlocal strain gradient constitutive law, higher-order boundary conditions of strain gradient theory as Eq. (19) are improperly adopted in the literature [76, 77].

3. Elastostatic torsion

Differences in the elastostatic torsional behavior of FG nano-beams are demonstrated adopting the nonlocal Lam strain gradient theory and the modified nonlocal strain gradient model to doubly clamped and cantilever nano-beams subjected to a uniformly distributed couples $\bar{q}_t$. To appropriately compare the size-dependent behavior of twisted FG elastic nano-beams, the effects corresponding to each gradient characteristic parameter in the NLSG are independently examined and compared with the counterpart results of MNSG. The non-dimensional parameters: axial abscissa $\bar{x}$, nonlocal characteristic parameter λ, gradient characteristic parameter μ, torsional rotation $\bar{\varphi}$ as well as the radius of gyration $\bar{r}$ are defined by

$$\bar{x}=\frac{x}{L},\qquad \lambda=\frac{L_c}{L},\qquad \mu=\frac{\ell}{L},\qquad \bar{\varphi}\left(\bar{x}\right)=\varphi\left(x\right)\frac{J_G}{\bar{q}_t L^2},\qquad \bar{r}=\frac{1}{L}\sqrt{\frac{J_G}{A_G}} \tag{23}$$

In the elastostatic analysis, the inertia term in the differential condition of equilibrium Eq. $(7)_1$ vanishes and the equilibrated twisting moment T has thus the expression

$$T\left(x\right)=-\int_a^x q_t\left(\zeta\right)d\zeta+\Upsilon_1 \tag{24}$$

up to the integration constant Υ_1. The torsional curvature κ is detected as a result of solving the constitutive differential equation of NLSG Eq. (16) or MNSG Eq. (21) in terms of integration constants Υ_2, Υ_3

$$\begin{aligned}\kappa\left(x\right)=&\,\Upsilon_2\exp\left(-x\sqrt{\frac{\alpha}{\beta}}\right)+\Upsilon_3\exp\left(x\sqrt{\frac{\alpha}{\beta}}\right)\\&+\frac{1}{2\sqrt{\alpha\beta}}\exp\left(-x\sqrt{\frac{\alpha}{\beta}}\right)\int_a^x\exp\left(\xi\sqrt{\frac{\alpha}{\beta}}\right)\left(T\left(\xi\right)-L_c^2\partial_{\xi\xi}T\left(\xi\right)\right)d\xi\\&-\frac{1}{2\sqrt{\alpha\beta}}\exp\left(x\sqrt{\frac{\alpha}{\beta}}\right)\int_a^x\exp\left(-\eta\sqrt{\frac{\alpha}{\beta}}\right)\left(T\left(\eta\right)-L_c^2\partial_{\eta\eta}T\left(\eta\right)\right)d\eta\end{aligned} \tag{25}$$

where α, β for NLSG and MNSG are defined as

$$\begin{aligned} \alpha\big|_{\text{NLSG}} &= J_G + 3A_G \ell_2^2, & \alpha\big|_{\text{MNSG}} &= J_G \\ \beta\big|_{\text{NLSG}} &= J_G \left(\frac{8}{15} \ell_1^2 + \frac{1}{4} \ell_2^2 \right), & \beta\big|_{\text{MNSG}} &= J_G \ell_s^2 \end{aligned} \tag{26}$$

The differential condition of kinematic compatibility $\kappa = \partial_x \varphi$ has to be subsequently integrated to detect the torsional rotation φ up to the integration constant Υ_4

$$\varphi(x) = \int_a^x \kappa(\zeta) d\zeta + \Upsilon_4 \tag{27}$$

The integration constants $\Upsilon_k \ (k = 1..4)$ can be evaluated by imposing two standard kinematic and static boundary conditions (BC) as well as the corresponding two CBCs associated with NLSG or MNSG. The proposed solution technique leads to exact analytical solutions by integrating differential equations of lower order. The acronyms LOC, NLSG and MNSG stand for local beam model, nonlocal Lam strain gradient model and modified nonlocal strain gradient model, respectively.

3.1. *Cantilever twisted FG nano-beam subjected to uniform couples*

The classical BC for a cantilever FG elastic nano-beam subjected to uniform couples write as

$$\varphi(a) = 0, \qquad T(b) = 0 \tag{28}$$

The non-dimensional torsional rotation of the cantilever beam is determined by applying the proposed solution technique while imposing the classical BCs and the corresponding CBCs. It may be shown that the maximum value of the torsional rotation of NLSG and MNSG is

$$\begin{aligned} \bar{\varphi}_{\max}^{\text{NLSG}} &= \left(\frac{1}{2} + \lambda \right) \frac{\bar{r}^2}{\bar{r}^2 + 3\mu_2^2} \\ \bar{\varphi}_{\max}^{\text{MNSG}} &= \frac{1}{2} + \lambda \end{aligned} \tag{29}$$

which means that the torsional rotation of the FG elastic nano-beam at the free end is independent of the gradient characteristic parameters μ_1 and μ_s for NLSG and MNSG, respectively. Accordingly, the value of the torsional rotation at the mid-span of the cantilever FG elastic beam is examined to analyze the effects of nonlocal and gradient characteristic parameters

$$\bar{\varphi}^{\mathrm{NLSG}}\Big|_{\bar{x}=\frac{1}{2}} = \frac{\bar{r}^2}{120\left(\bar{r}^2+3\mu_2^2\right)^2}\Big(45\bar{r}^2+120\lambda\bar{r}^2+120\lambda^2\bar{r}^2-64\bar{r}^2\mu_1^2+135\mu_2^2+360\lambda\mu_2^2+360\lambda^2\mu_2^2 \\ -30\bar{r}^2\mu_2^2-2\operatorname{sech}\left(\frac{1}{\bar{r}}\sqrt{\frac{15\left(\bar{r}^2+3\mu_2^2\right)}{32\mu_1^2+15\mu_2^2}}\right)\left(30\lambda\left(1+2\lambda\right)\left(\bar{r}^2+3\mu_2^2\right)-\bar{r}^2\left(32\mu_1^2+15\mu_2^2\right)\right)\Big) \tag{30}$$

$$\bar{\varphi}^{\mathrm{MNSG}}\Big|_{\bar{x}=\frac{1}{2}} = \frac{1}{8}\left(3+8\lambda\left(1+\lambda\right)-8\mu_s^2-4\left(\lambda+2\lambda^2-2\mu_s^2\right)\operatorname{sech}\left(\frac{1}{2\mu_s}\right)\right)$$

3.2. *Doubly clamped FG nano-beam subjected to uniform couples*

For a FG elastic nano-beam subjected to uniform couples with doubly clamped ends, the kinematic BCs are given by

$$\varphi(a)=0, \qquad \varphi(b)=0 \tag{31}$$

The non-dimensional torsional rotation can be detected exploiting the proposed solution methodology and prescribing the kinematic BCs and the CBCs. For numerical illustrations, the maximum non-dimensional torsional rotation is determined as

$$\bar{\varphi}_{\max}^{\mathrm{NLSG}} = \frac{\bar{r}^2}{120\left(\bar{r}^2+3\mu_2^2\right)^2}\Big(15\bar{r}^2+60\lambda\bar{r}^2+120\lambda^2\bar{r}^2-64\bar{r}^2\mu_1^2+45\mu_2^2+180\lambda\mu_2^2+360\lambda^2\mu_2^2 \\ -30\bar{r}^2\mu_2^2-2\operatorname{sech}\left(\frac{1}{\bar{r}}\sqrt{\frac{15\left(\bar{r}^2+3\mu_2^2\right)}{32\mu_1^2+15\mu_2^2}}\right)\left(30\lambda\left(1+2\lambda\right)\left(\bar{r}^2+3\mu_2^2\right)-\bar{r}^2\left(32\mu_1^2+15\mu_2^2\right)\right)\Big) \tag{32}$$

$$\bar{\varphi}_{\max}^{\mathrm{MNSG}} = \frac{1}{8}\left(1+4\lambda+8\lambda^2-8\mu_s^2-4\left(\lambda+2\lambda^2-2\mu_s^2\right)\operatorname{sech}\left(\frac{1}{2\mu_s}\right)\right)$$

3.3. *Numerical results of elastostatic torsion*

The normalized torsional rotations at the mid-span of the FG elastic nano-beams associated with the nonlocal Lam strain gradient model are illustrated in Figs. 2-5 for cantilever and doubly clamped beams subjected to uniformly distributed couples. The effects of stretch and rotation gradient parameters in the framework of nonlocal Lam strain gradient model are separately examined and the results consistent with the NLSG with $\ell_1 \neq 0$ are compared with the counterpart results of the modified nonlocal strain gradient model. The demonstrated torsional rotation $\bar{\varphi}$ is normalized with respect to the corresponding torsional rotation of the local beam model $\bar{\varphi}^{\mathrm{LOC}}$. In Figs. 2-3 where 2D comparison is made between the torsional response of NLSG (with $\ell_1 \neq 0$) and MNSG beams, the nonlocal characteristic parameter λ is ranging in the interval $]0,1[$. The stretch gradient parameter of NLSG μ_1 and gradient characteristic parameter of MNSG μ_s are ranging in the set of $\{0.1, 0.3, 0.5, 0.7, 1.0\}$ while the rotation gradient parameter of NLSG μ_2 is assumed to vanish. Figs. 4 and 5 demonstrate the 3D variations of normalized torsional rotation at the mid-span of the FG elastic nano-beam versus the nonlocal characteristic parameters where the effects of stretch and rotation gradient parameters are independently investigated. All the characteristic parameters in Figs. 4 and 5 are ranging in the interval $]0,1[$. Furthermore, in all of the illustrated results associated with NLSG, the non-dimensional radius of gyration is assumed as $\bar{r} = 1/10\sqrt{2}$.

It is noticeably deduced from Figs. 2-5 that the adopted size-dependent NLSG and MNSG models exhibit a softening behavior in terms of the nonlocal characteristic parameter λ, that is a larger λ involves a larger torsional rotation for a given gradient characteristic parameter. The torsional rotation of FG elastic nano-beam also decreases as the gradient parameters increase, and accordingly, both nonlocal strain gradient theories demonstrate a stiffening behavior in terms of the gradient parameters for a given value of λ. Notably, the torsional

response of nano-beams associated with both NLSG and MNSG models are in full agreement as the gradient characteristic parameters tend to zero. While the torsional response of nano-beam associated with the MNSG underestimates the counterpart torsional rotation of NLSG beam with non-vanishing stretch gradient parameter μ_1, it is strictly higher than the torsional rotation of NLSG beam with non-vanishing rotation gradient parameter μ_2. This is clearly due to the dominant stiffening effects of rotation gradient parameter μ_2 in comparison to stretch gradient parameter μ_1 in NLSG. As expected, the size-dependent elastic torsional rotation of nano-beams in accordance with either of the nonlocal strain gradient models coincides with the local response for vanishing nonlocal and gradient parameters.

The numerical values of normalized maximum and mid-span torsional rotation of doubly clamped and cantilever FG elastic nano-beams examined in the framework of NLSG and MNSG are, respectively, collected in Tables 1-2 and 3-4.

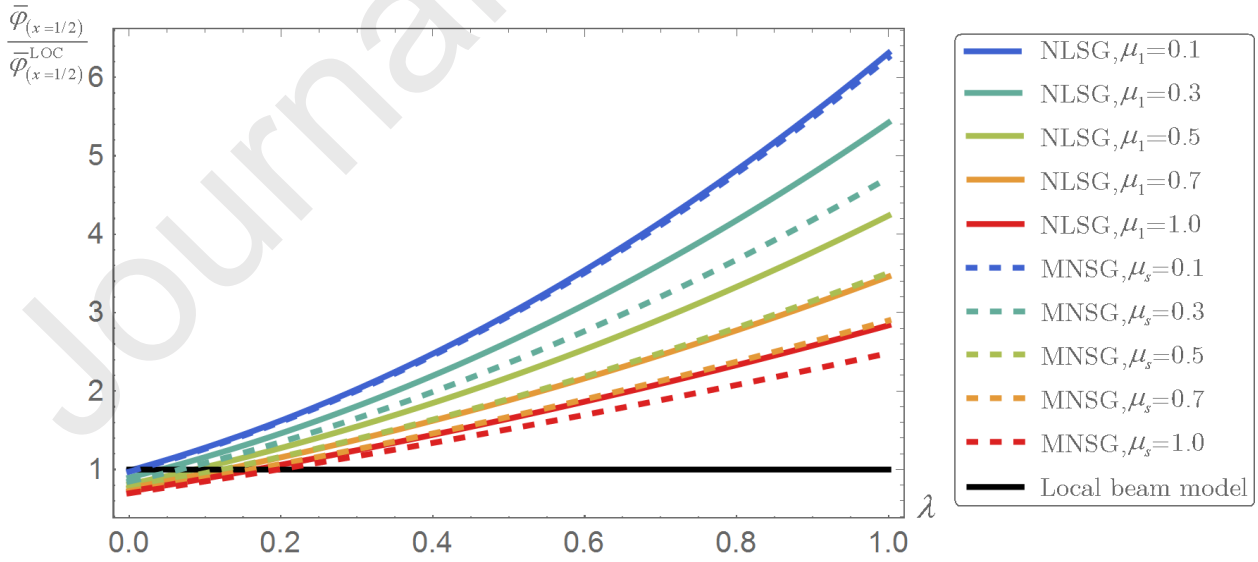

Fig. 2. Cantilever FG nano-beams under uniform couples: normalized mid-span torsional rotation $\bar{\varphi}_{(x=1/2)}$ versus nonlocal and gradient parameters by NLSG $(\ell_1 \neq 0)$ and MNSG

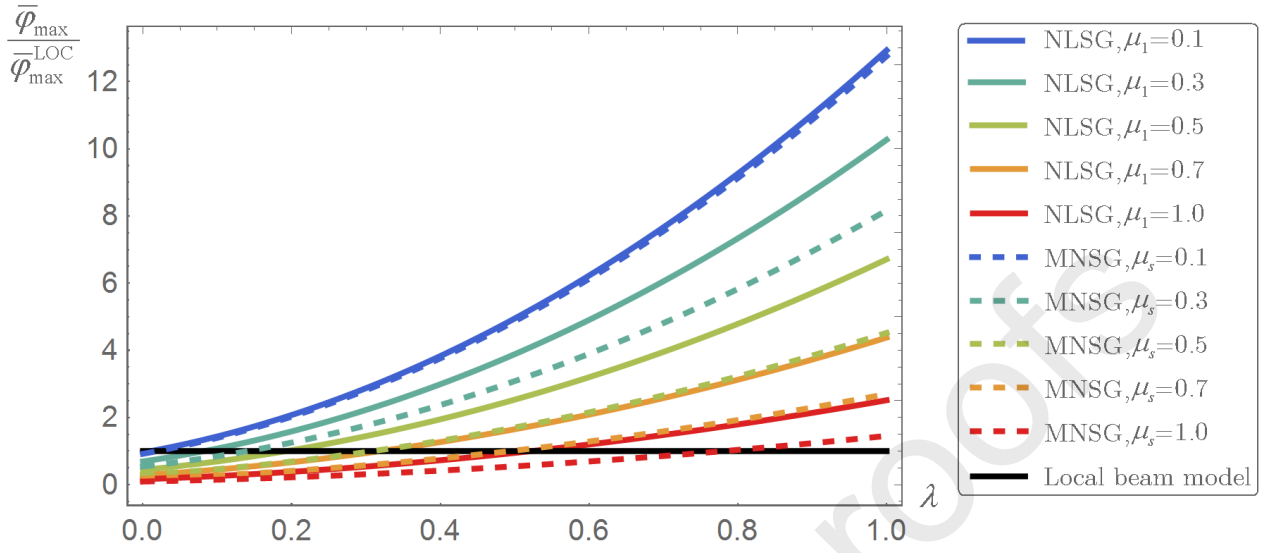

Fig. 3. Doubly clamped FG nano-beams under uniform couples: normalized maximum torsional rotation $\overline{\varphi}_{\max}$ versus nonlocal and gradient parameters by NLSG $(\ell_1 \neq 0)$ and MNSG

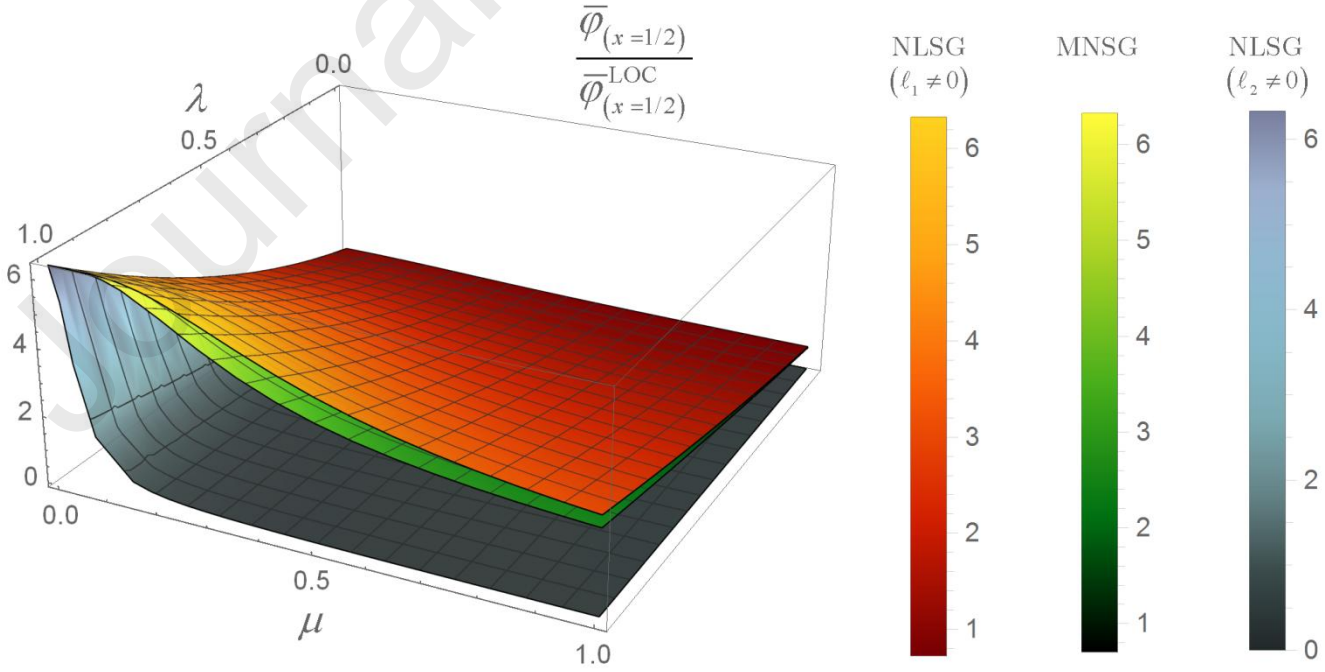

Fig. 4. Uniformly loaded cantilever FG nano-beams: effects of λ, μ on normalized $\bar{\varphi}_{(x=1/2)}$ by

$\mathrm{NLSG}(\ell_1 \neq 0)$, $\mathrm{NLSG}(\ell_2 \neq 0)$ and MNSG

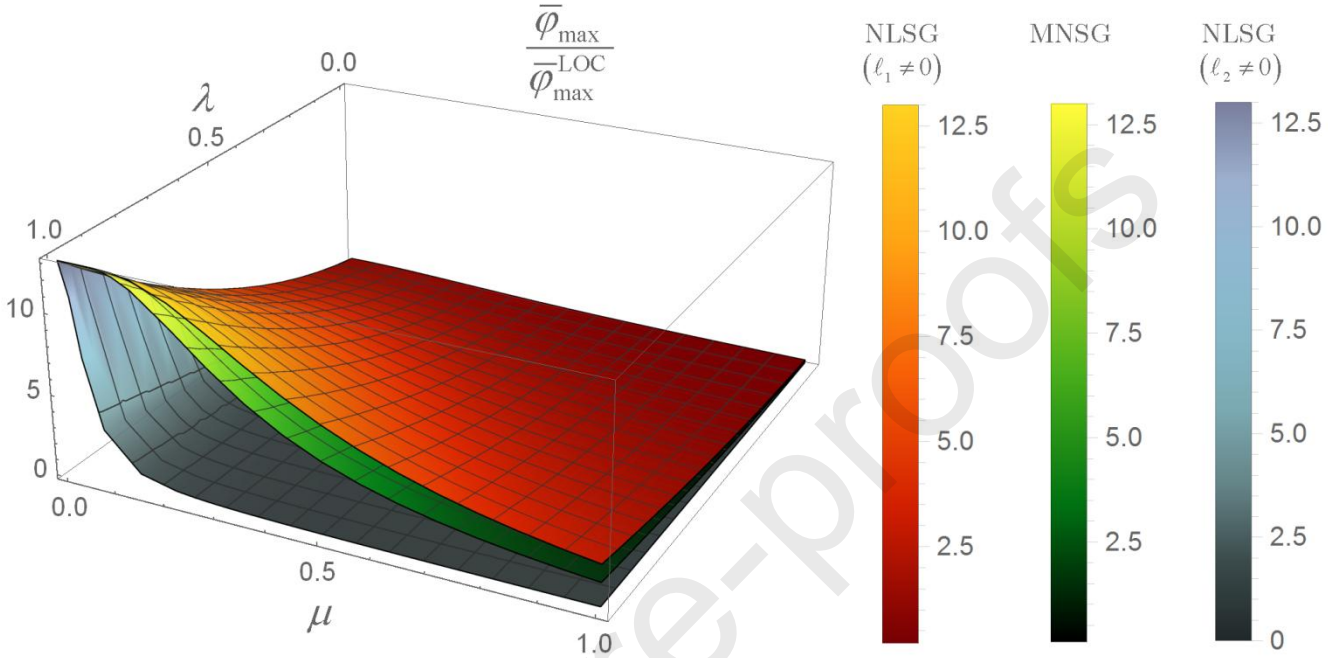

Fig. 5. Uniformly loaded doubly clamped FG nano-beams: effects of λ, μ on normalized

$\bar{\varphi}_{\max}$ by $\mathrm{NLSG}(\ell_1 \neq 0)$, $\mathrm{NLSG}(\ell_2 \neq 0)$ and MNSG

4. Torsional elastic vibrations

4.1. *Free vibration analysis*

To examine the torsional free vibrations of FG elastic nano-beams, applied distributed torsional couples are assumed to vanish in the differential condition of equilibrium. The twisting moment T is detected by applying the differential condition of equilibrium Eq. $(7)_1$ to the constitutive differential law of NLSG Eq. (16) as

$$T = J_\rho L_c^2 \partial_{xtt}\varphi + \left(J_G + 3A_G \ell_2^2\right)\kappa - J_G\left(\frac{8}{15}\ell_1^2 + \frac{1}{4}\ell_2^2\right)\partial_{xx}\kappa \tag{33}$$

Employing the kinematic compatibility $\kappa = \partial_x \varphi$, the differential condition of dynamic equilibrium governing the torsional vibrations is consequently given by

$$J_\rho \partial_{tt}\varphi - J_\rho L_c^2 \partial_{xxtt}\varphi = \left(J_G + 3A_G \ell_2^2\right)\partial_{xx}\varphi - J_G\left(\frac{8}{15}\ell_1^2 + \frac{1}{4}\ell_2^2\right)\partial_{xxxx}\varphi \tag{34}$$

equipped with the classical boundary conditions Eq. $(7)_2$ and corresponding constitutive boundary conditions of NLSG Eq. (17). A well-established procedure of separating spatial and time variables is then utilized to analyze the relevant vibrational problem

$$\varphi(x,t) = \Phi(x)\exp(i\omega t) \tag{35}$$

where $i = \sqrt{-1}$, Φ and ω are the torsional mode shapes and natural frequency of vibrations. The governing equation of the torsional coordinate function Φ can be obtained by enforcing the separation of variables Eq. (35) to the differential condition of dynamic equilibrium Eq. (34)

$$J_G\left(\frac{8}{15}\ell_1^2 + \frac{1}{4}\ell_2^2\right)\frac{d^4\Phi}{dx^4} + \left(J_\rho L_c^2\omega^2 - \left(J_G + 3A_G\ell_2^2\right)\right)\frac{d^2\Phi}{dx^2} - J_\rho\omega^2\Phi = 0 \tag{36}$$

The torsional coordinate function can be analytically detected as

$$\Phi(x) = \Gamma_1 \sin\zeta_1 x + \Gamma_2 \cos\zeta_1 x + \Gamma_3 \sinh\zeta_2 x + \Gamma_4 \cosh\zeta_2 x \tag{37}$$

where the unknown constants $\Gamma_k\ (k = 1..4)$ are determined by prescribing suitable classical and constitutive boundary conditions, along with

$$\begin{aligned}\zeta_1^2 &= \frac{\left(J_\rho L_c^2\omega^2 - \alpha\right) + \sqrt{\left(J_\rho L_c^2\omega^2 - \alpha\right)^2 + 4J_\rho\omega^2\beta}}{2\beta}\\ \zeta_2^2 &= \frac{-\left(J_\rho L_c^2\omega^2 - \alpha\right) + \sqrt{\left(J_\rho L_c^2\omega^2 - \alpha\right)^2 + 4J_\rho\omega^2\beta}}{2\beta}\end{aligned} \tag{38}$$

with α, β introduced for NLSG and MNSG as Eq. (26).

To illustrate the solution procedure for detecting the torsional natural frequency of FG elastic nano-beam, let us consider a cantilever FG nano-beam in the nonlocal Lam strain gradient theory. A homogeneous fourth-order algebraic system in terms of the unknown constants $\Gamma_k \ (k=1..4)$ is formulated by prescribing the classical BC Eq. (28) along with the CBC Eq. (17) in the torsional coordinate function Eq. (37). Similarly, homogeneous fourth-order algebraic systems can be detected for nano-beams associated with either of nonlocal strain gradient models of NLSG or MNSG. To detect the non-trivial solution of torsional free vibrations, the system of algebraic equations has to be singular, that is the determinant of the coefficients of the homogeneous system has to vanish. For cantilever and doubly clamped FG elastic beams consistent with either of the nonlocal strain gradient models, a highly nonlinear characteristic equation in terms of torsional natural frequencies is found that is numerically solved.

4.2. *Numerical results of torsional free vibrations*

Torsional natural frequency of cantilever and doubly clamped FG elastic nano-beams in the framework of nonlocal Lam strain gradient theory and modified nonlocal strain gradient model are numerically evaluated here. The effects of stretch and rotation gradient parameters associated with NLSG are separately examined and the results consistent with NLSG with $\ell_1 \neq 0$ are compared with the counterpart results of the MNSG. For consistency, the non-dimensional torsional fundamental frequency $\bar{\omega}$ is introduced in the illustrations as

$$\bar{\omega}^2 = \left(\frac{L^2 J_\rho}{\pi^2 J_G} \right) \omega^2 \tag{39}$$

The illustrated torsional fundamental frequencies are furthermore normalized employing their corresponding local counterparts $\bar{\omega}_{\mathrm{LOC}}$.

The effects of characteristic parameters on the normalized fundamental frequency of the nonlocal Lam strain gradient model with non-vanishing stretch gradient parameters $\ell_1 \neq 0$ in comparison with the counterpart results of the modified nonlocal strain gradient model are exhibited in Figs. 6 and 7 for cantilever and doubly clamped FG nano-beams. The variations of the normalized torsional frequencies associated with the nonlocal Lam strain gradient model with non-vanishing rotation gradient parameters $\ell_2 \neq 0$ are depicted in Figs. 8 and 9. The nonlocal and gradient characteristic parameters in Figs. 6 and 7 are considered to range in the same set as the elastostatic torsional response illustrated in Figs. 2-3. Also in the results consistent with NLSG with $\ell_2 \neq 0$, as illustrated in Fig. 8 and 9, the rotation gradient parameter μ_2 is ranging in the set of $\{0.01, 0.1, 0.3, 0.5, 0.7, 1.0\}$, the nonlocal parameter λ is ranging in the interval $]0,1[$ and the stretch gradient parameter μ_1 is assumed to vanish. It is inferred from the outcomes in Figs. 6-9 that the torsional fundamental frequencies in accordance with both the NLSG and MNSG models decrease as the nonlocal characteristic parameters λ increases, and thus, exhibits a softening behavior in terms of the nonlocal characteristic parameter λ for a given value of μ. The gradient parameters μ have the effect of increasing the fundamental torsional frequencies that is a larger μ involves a larger fundamental frequency for a given value of λ. Therefore, the fundamental frequencies associated with both the NLSG and MNSG models exhibit a stiffening behavior in terms of the gradient parameters μ. Remarkably, while the torsional fundamental frequencies of nano-beam associated with the MNSG overestimates the counterpart natural frequencies of NLSG beam with non-vanishing stretch gradient parameter μ_1, it is strictly lower than the torsional frequencies of NLSG beam with non-vanishing rotation gradient parameter μ_2. This is noticeably occurred as a result of dominant stiffening effects of the rotation gradient parameter μ_2 compared with the stretch gradient parameter μ_1 in the framework of NLSG.

As predictable, the torsional fundamental frequency of local elastic beam model is recovered for vanishing nonlocal and gradient parameters.

Numerical values of normalized torsional fundamental frequencies detected in the framework of the nonlocal Lam strain gradient theory and modified nonlocal strain gradient model for doubly clamped and cantilever FG elastic beams are correspondingly reported in Tables 5-6 and 7-8.

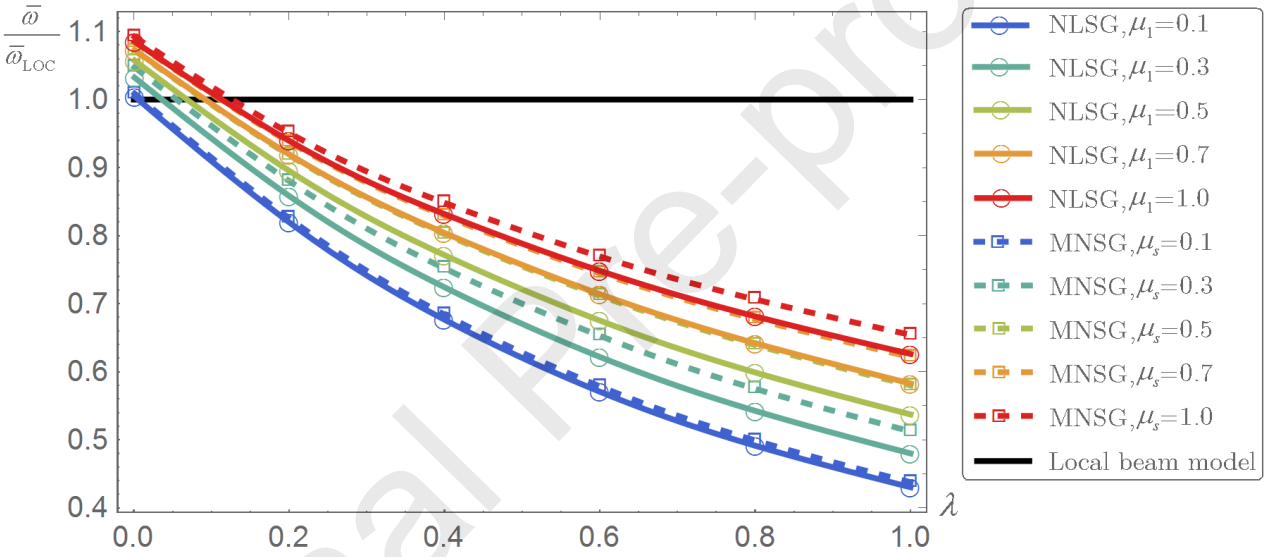

Fig. 6. Normalized torsional fundamental frequency of cantilever FG nano-beams by NLSG $(\ell_1 \neq 0)$ and MNSG

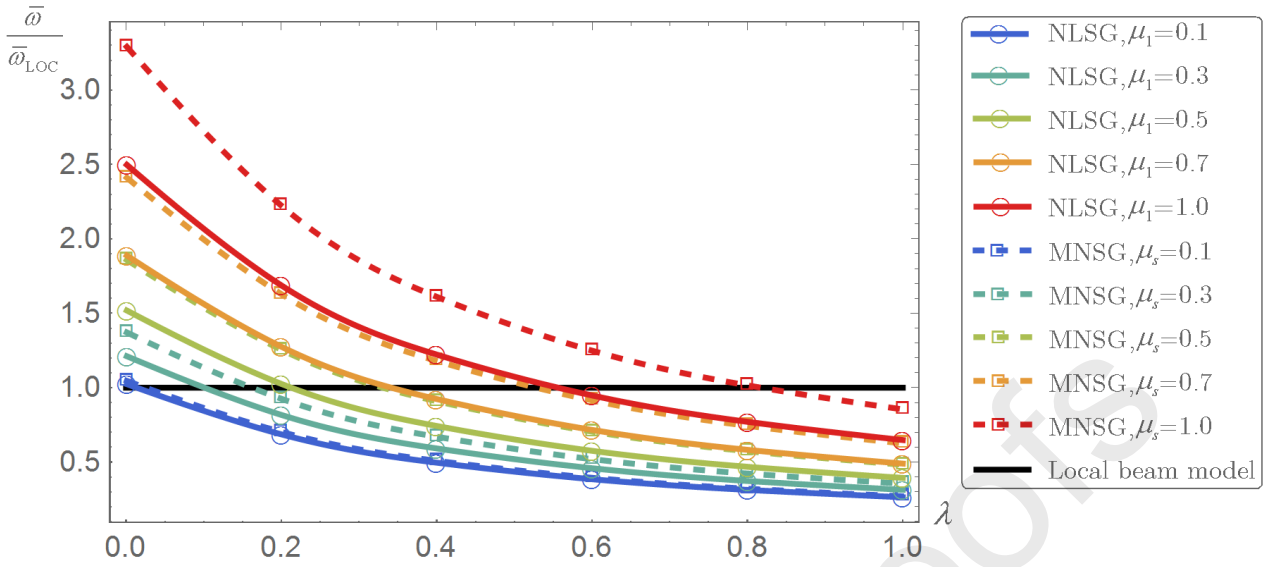

Fig. 7. Normalized torsional fundamental frequency of doubly clamped FG nano-beams by NLSG$\left(\ell_1 \neq 0\right)$ and MNSG

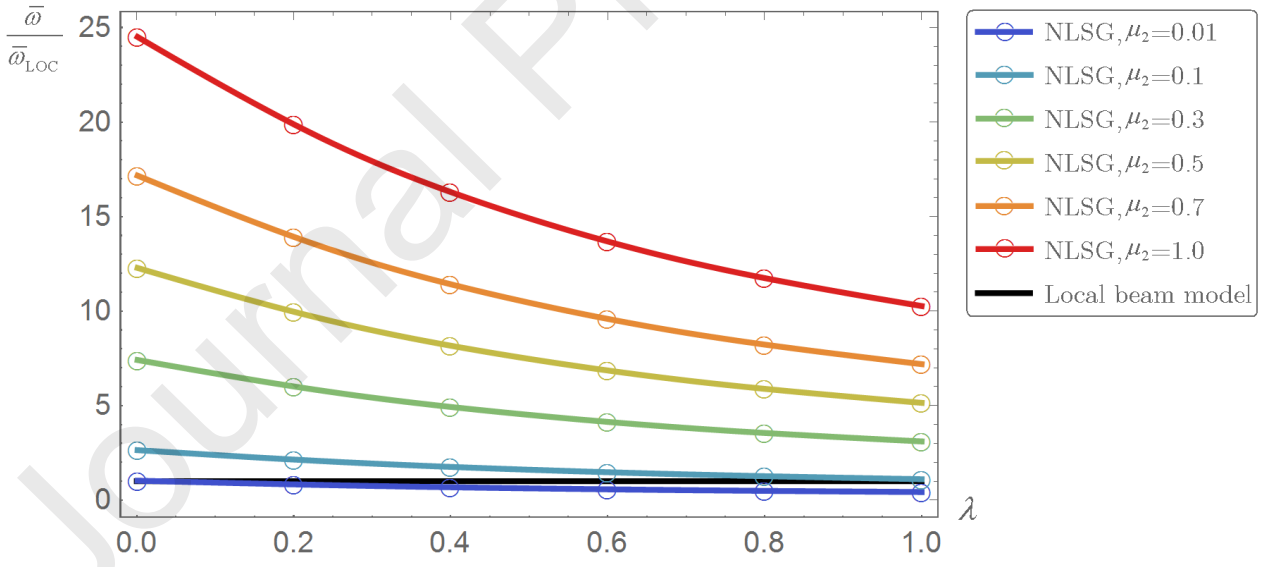

Fig. 8. Effects of characteristic parameters on the normalized torsional frequency of cantilever FG nano-beams by NLSG$\left(\ell_2 \neq 0\right)$

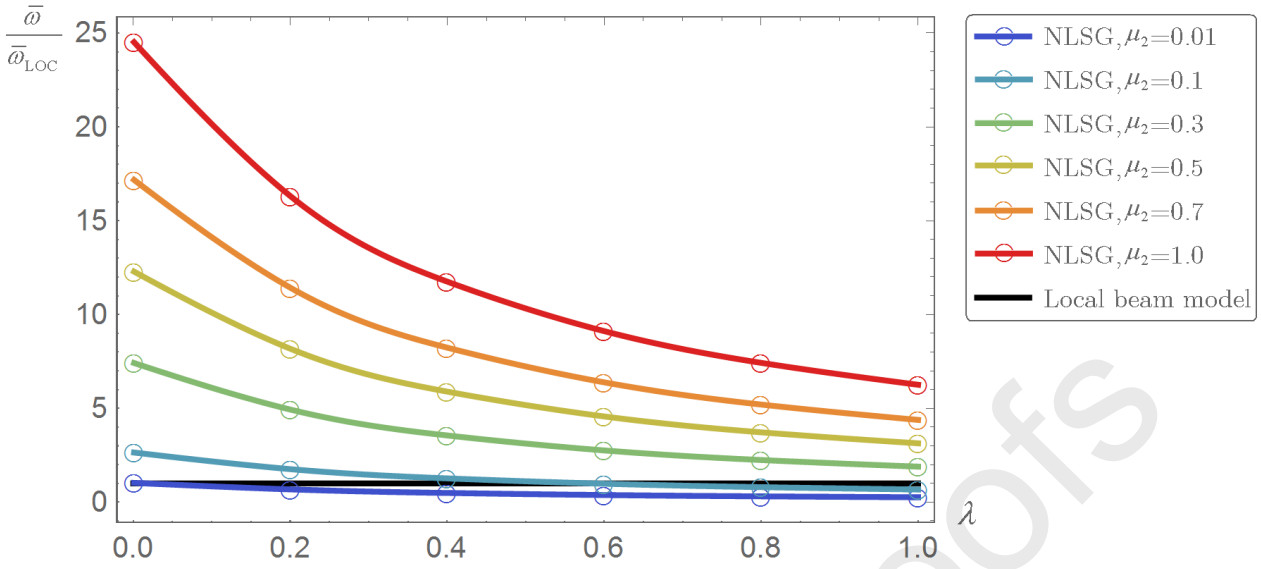

Fig. 9. Effects of characteristic parameters on the normalized torsional frequency of doubly clamped FG nano-beams by NLSG$\left(\ell_2 \neq 0\right)$

5. Conclusions

As a result of unifying Eringen's nonlocal integral theory and modified strain gradient theory, the nonlocal Lam strain gradient model has been formulated in the present study to examine elasto-static and –dynamic torsional behaviors of FG elastic nano-beams. Three characteristic parameters including two gradient parameters associated with the nano-structure stretch and rotation gradients as well as one nonlocal characteristic parameter, reflecting long-range nonlocal interactions, have been introduced in the nonlocal Lam strain gradient theory.

A variationally consistent constitutive formulation has been conceived, proving thus well-posed torsional problems of FG elastic nano-beams. The nonlocal Lam strain gradient model has been shown to be governed by integral convolutions, conveniently revertible to differential equations equipped with non-classical constitutive boundary conditions. It has been demonstrated that for vanishing nonlocal parameter, the gradient law and non-standard boundary conditions of the modified strain gradient theory are recovered.

Torsional elastostatic rotations and natural frequencies of FG elastic nano-beams have been evaluated utilizing an efficient analytical approach and new numerical benchmarks have been detected. Both softening and stiffening torsional responses can be effectively described in the innovative framework of the novel nonlocal Lam strain gradient model which provides thus an effective approach for design and optimization of structural elements of modern NEMS.

The presented nonlocal Lam strain gradient methodology has been tested by comparing the elasto-static and –dynamic torsional responses of FG elastic nano-beams with the results obtained by the modified nonlocal strain gradient theory.

The main outcomes can be enumerated as follows.

- Elastostatic rotations and torsional natural frequencies of FG elastic nano-beams associated with the nonlocal Lam strain gradient elasticity theory expose softening and stiffening torsional behaviors in terms of the nonlocal and gradient parameters, respectively.
- The torsional response of FG elastic nano-beams consistent with the nonlocal Lam strain gradient model is coincident with the counterpart results associated with the modified nonlocal strain gradient model as the gradient characteristic parameters tend to zero.
- The elastostatic torsional response of FG elastic nano-beams associated with the modified nonlocal strain gradient model underestimates the counterpart results consistent with the nonlocal Lam strain gradient theory with non-vanishing stretch gradient parameter. Torsional elastic rotations of nonlocal Lam strain gradient beams with non-vanishing rotation gradient parameter are instead overestimated.
- The torsional fundamental frequency of FG elastic nano-beam associated with the modified nonlocal strain gradient model is strictly higher than the counterpart natural frequency obtained by nonlocal Lam strain gradient theory with non-vanishing stretch

gradient parameter. It is strictly lower than the torsional frequency of nonlocal Lam strain gradient beam with non-vanishing rotation gradient parameter.

- In nonlocal Lam strain gradient elasticity, the stiffening effect of the rotation gradient parameter is more noticeable in comparison with the stretch gradient parameter.
- Torsional elastostatic rotations and fundamental frequencies of local FG elastic beam are recovered as the nonlocal and gradient characteristic parameters tend to zero.

Acknowledgement

The financial support of the Italian Ministry for University and Research (P.R.I.N. National Grant 2017, Project code 2017J4EAYB; "University of Naples Federico II" Research Unit) is gratefully acknowledged.

References

1. Zhang W, Obitani K, Hirai Y, Tsuchiya T, Tabata O. Fracture strength of silicon torsional mirror resonators fully coated with submicrometer-thick PECVD DLC film. Sens Actuators A 2019; 286: 28-34. https://doi.org/10.1016/j.sna.2018.12.021
2. Xiao D, Li Q, Hou Z, Xia D, Xu X, Wu X. A double differential torsional micro-accelerometer based on V-shape beam. Sens Actuators A 2017; 258: 182-192. https://doi.org/10.1016/j.sna.2017.03.011
3. Laurent L, Yon JJ, Moulet JS, Imperinetti P, Duraffourg L. Compensation of nonlinear hardening effect in a nanoelectromechanical torsional resonator. Sens Actuators A 2017; 263: 326-331. https://doi.org/10.1016/j.sna.2017.06.027

4. Sedighi HM, Koochi A, Keivani M, Abadyan M. Microstructure-dependent dynamic behavior of torsional nano-varactor Meas 2017; 111: 114-121. https://doi.org/10.1016/j.measurement.2017.07.011
5. Laghi G, Dellea S, Longoni A, Minotti P, Tocchio A, Zerbini S, Langfelder G. Torsional MEMS magnetometer operated off-resonance for in-plane magnetic field detection. Sens Actuators A 2015; 229: 218-226. https://doi.org/10.1016/j.sna.2015.01.027
6. Xiao GJ, Pan CL, Liu YB, Feng ZH. In-plane torsion of discal piezoelectric actuators with spiral interdigitated electrodes. Sens Actuators A 2015; 227: 1-10. https://doi.org/10.1016/j.sna.2015.03.042
7. Shen JP, Wang PY, Li C, Wang YY. New observations on transverse dynamics of microtubules based on nonlocal strain gradient theory. Compos Struct 2019; 225: 111036. https://doi.org/10.1016/j.compstruct.2019.111036.
8. Şimşek M. Some closed-form solutions for static, buckling, free and forced vibration of functionally graded (FG) nanobeams using nonlocal strain gradient theory. Compos Struct 2019; 224: 111041. https://doi.org/10.1016/j.compstruct.2019.111041.
9. Shiva K, Raghu P, Rajagopal A, Reddy JN. Nonlocal buckling analysis of laminated composite plates considering surface stress effects. Compos Struct 2019; 226: 111216. https://doi.org/10.1016/j.compstruct.2019.111216
10. Zhu J, Lv Z, Liu H. Thermo-electro-mechanical vibration analysis of nonlocal piezoelectric nanoplates involving material uncertainties. Compos Struct 2019; 208: 771-783. https://doi.org/10.1016/j.compstruct.2018.10.059.
11. Liu H, Lv Z, Wu H. Nonlinear free vibration of geometrically imperfect functionally graded sandwich nanobeams based on nonlocal strain gradient theory. Compos Struct 2019; 214: 47-61. https://doi.org/10.1016/j.compstruct.2019.01.090.

12. Zhao B, Chen J, Liu T, Song W, Zhang J. A new Timoshenko beam model based on modified gradient elasticity: Shearing effect and size effect of micro-beam. Compos Struct 2019; 223: 110946.https://doi.org/10.1016/j.compstruct.2019.110946.
13. Goncalves BR, Karttunen AT, Romanoff J. A nonlinear couple stress model for periodic sandwich beams. Compos Struct 2019; 212: 586-597. https://doi.org/10.1016/j.compstruct.2019.01.034
14. Mollamahmutoğlu Ç, Mercan A. A novel functional and mixed finite element analysis of functionally graded micro-beams based on modified couple stress theory. Compos Struct 2019; 223: 110950. https://doi.org/10.1016/j.compstruct.2019.110950.
15. Repka M, Sladek V, Sladek J. Numerical study of size effects in micro/nano plates by moving finite elements. Compos Struct 2019; 212: 291-303. https://doi.org/10.1016/j.compstruct.2019.01.010.
16. Baltacıoğlu AK, Civalek Ö. Vibration analysis of circular cylindrical panels with CNT reinforced and FGM composites. Compos Struct 2018; 202: 374-388. https://doi.org/10.1016/j.compstruct.2018.02.024.
17. Momeni SA, Asghari M. The second strain gradient functionally graded beam formulation. Compos Struct 2018; 188: 15-24. https://doi.org/10.1016/j.compstruct.2017.12.046
18. Barretta R, Faghidian SA, Marotti de Sciarra F. Aifantis versus Lam strain gradient models of Bishop elastic rods. Acta Mech 2019; 230: 2799–2812. https://doi.org/10.1007/s00707-019-02431-w
19. Barretta R, Čanađija M, Marotti de Sciarra F. Nonlocal integral thermoelasticity: A thermodynamic framework for functionally graded beams. Compos Struct 2019; 225: 111104. https://doi.org/10.1016/j.compstruct.2019.111104.

20. Barretta R, Marotti de Sciarra F. Variational nonlocal gradient elasticity for nano-beams. Int J Eng Sci 2019; 143: 73-91. https://doi.org/10.1016/j.ijengsci.2019.06.016.

21. Romano G, Barretta R, Diaco M. Iterative methods for nonlocal elasticity problems. Continuum Mech Thermodyn 2019; 31: 669–689. https://doi.org/10.1007/s00161-018-0717-8

22. Ouakad HM, Sedighi HM. Static response and free vibration of MEMS arches assuming out-of-plane actuation pattern. Int J Non Linear Mech 2019; 110: 44-57. https://doi.org/10.1016/j.ijnonlinmec.2018.12.011

23. Shirbani MM, Sedighi HM, Ouakad HM, Najar F. Experimental and mathematical analysis of a piezoelectrically actuated multilayered imperfect microbeam subjected to applied electric potential. Compos Struct 2018; 184: 950-960. https://doi.org/10.1016/j.compstruct.2017.10.062

24. Shishesaz M, Shirbani MM, Sedighi HM, Hajnayeb A. Design and analytical modeling of magneto-electro-mechanical characteristics of a novel magneto-electro-elastic vibration-based energy harvesting system. J Sound Vib 2018; 425: 149-169. https://doi.org/10.1016/j.jsv.2018.03.030

25. She G-L, Ren Y-R, Yuan F-G. Hygro-thermal wave propagation in functionally graded double-layered nanotubes systems. Steel Compos Struct 2019; 31: 641-653. http://dx.doi.org/10.12989/scs.2019.31.6.641.

26. She G-L, Yuan F-G, Ren Y-R. On wave propagation of porous nanotubes. Int J Eng Sci 2018; 130: 62–74. https://doi.org/10.1016/j.ijengsci.2018.05.002

27. She G-L, Yuan F-G, Ren Y-R, Liu H-B, Xiao W-S. Nonlinear bending and vibration of functionally graded porous tubes via a nonlocal strain gradient theory. Compos Struct 2017; 89: 160-169. https://doi.org/10.1016/j.physe.2017.01.027.

28. Shen JP, Li C. A semi-continuum-based bending analysis for extreme-thin micro/nano-beams and new proposal for nonlocal differential constitution. Compos Struct 2017; 172: 210-220. https://doi.org/10.1016/j.compstruct.2017.03.070.
29. Li C, Li S, Yao L, Zhu Z. Nonlocal theoretical approaches and atomistic simulations for longitudinal free vibration of nanorods/nanotubes and verification of different nonlocal models. Appl Math Modell 2015; 39: 4570-4585. https://doi.org/10.1016/j.apm.2015.01.013.
30. Thai H-T, Vo TP, Nguyen T-K, Kim S-E. A review of continuum mechanics models for size-dependent analysis of beams and plates. Compos Struct 2017; 177: 196-219. https://doi.org/10.1016/j.compstruct.2017.06.040.
31. Ghayesh MH, Farajpour A. A review on the mechanics of functionally graded nanoscale and microscale structures. Int J Eng Sci 2019; 137: 8-36. https://doi.org/10.1016/j.ijengsci.2018.12.001
32. Eringen A. On differential equations of nonlocal elasticity and solutions of screw dislocation and surface waves. J Appl Phys 1983; 54: 4703–4710. https://doi.org/10.1063/1.332803
33. Romano G, Barretta R, Diaco M, Marotti de Sciarra F. Constitutive boundary conditions and paradoxes in nonlocal elastic nano-beams. Int J Mech Sci 2017; 121: 151-156. https://doi.org/10.1016/j.ijmecsci.2016.10.036
34. Romano G, Barretta R, Diaco M. On nonlocal integral models for elastic nanobeams. Int J Mech Sci 2017; 131: 490-499. https://doi.org/10.1016/j.ijmecsci.2017.07.013
35. Romano G, Luciano R, Barretta R, Diaco M. Nonlocal integral elasticity in nanostructures, mixtures, boundary effects and limit behaviours. Continuum Mech Thermodyn 2018; 30: 641–655. https://doi.org/10.1007/s00161-018-0631-0

36. Romano G, Barretta R. Nonlocal elasticity in nanobeams: the stress-driven integral model. Int J Eng Sci 2017; 115: 14–27. https://doi.org/10.1016/j.ijengsci.2017.03.002

37. Romano G, Barretta R. Stress-driven versus strain-driven nonlocal integral model for elastic nano-beams. Compos Part B 2017; 114: 184–188. https://doi.org/10.1016/j.compositesb.2017.01.008

38. Barretta R, Fazelzadeh SA, Feo L, Ghavanloo E, Luciano R. Nonlocal inflected nano-beams: A stress-driven approach of bi-Helmholtz type. Compos Struct 2018; 200: 239-245. https://doi.org/10.1016/j.compstruct.2018.04.072.

39. Barretta R, Čanađija M, Luciano R, Marotti de Sciarra F. Stress-driven modeling of nonlocal thermoelastic behavior of nanobeams. Int J Eng Sci 2018; 126: 53-67. https://doi.org/10.1016/j.ijengsci.2018.02.012

40. Barretta R, Marotti de Sciarra F, Vaccaro MS. On nonlocal mechanics of curved elastic beams. Int J Eng Sci 2019; 144, 103140. https://doi.org/10.1016/j.ijengsci.2019.103140.

41. Barretta R, Fabbrocino F, Luciano R, Marotti de Sciarra F. Closed-form solutions in stress-driven two-phase integral elasticity for bending of functionally graded nano-beams. Physica E 2018; 97: 13-30. https://doi.org/10.1016/j.physe.2017.09.026

42. Barretta R, Caporale A, Faghidian SA, Luciano R, Marotti de Sciarra F, Medaglia CM. A stress-driven local-nonlocal mixture model for Timoshenko nano-beams. Compos Part B 2019; 164: 590-598. https://doi.org/10.1016/j.compositesb.2019.01.012

43. Barretta R, Faghidian SA, Marotti de Sciarra F. Stress-driven nonlocal integral elasticity for axisymmetric nano-plates. Int J Eng Sci 2019; 136: 38-52. https://doi.org/10.1016/j.ijengsci.2019.01.003

44. Barretta R, Fabbrocino F, Luciano R, Marotti de Sciarra F, Ruta G. Buckling loads of nano-beams in stress-driven nonlocal elasticity. Mech Adv Mater Struct 2019. https://doi.org/10.1080/15376494.2018.1501523

45. Apuzzo A, Barretta R, Luciano R, Marotti de Sciarra F, Penna R. Free vibrations of Bernoulli-Euler nano-beams by the stress-driven nonlocal integral model. Compos Part B 2017; 123: 105–111. https://doi.org/10.1016/j.compositesb.2017.03.057
46. Barretta R, Faghidian SA, Luciano R, Medaglia CM, Penna R. Free vibrations of FG elastic Timoshenko nano-beams by strain gradient and stress driven nonlocal models. Compos Part B 2018; 154: 20-32. https://doi.org/10.1016/j.compositesb.2018.07.036
47. Mahmoudpour E, Hosseini-Hashemi SH, Faghidian SA. Non-linear vibration analysis of FG nano-beams resting on elastic foundation in thermal environment using stress-driven nonlocal integral model. Appl Math Modell 2018; 57: 302-315. https://doi.org/10.1016/j.apm.2018.01.021
48. Apuzzo A, Barretta R, Fabbrocino F, Faghidian SA, Luciano R, Marotti de Sciarra F. Axial and torsional free vibrations of elastic nano-beams by stress-driven two-phase elasticity. Appl Comput Mech 2019; 5: 402-413. https://doi.org/10.22055/jacm.2018.26552.1338
49. Barretta R, Faghidian SA, Luciano R. Longitudinal vibrations of nano-rods by stress-driven integral elasticity. Mech Adv Mater Struct 2019; 26: 1307–1315. https://doi.org/10.1080/15376494.2018.1432806
50. Mindlin RD. Second gradient of strain and surface-tension in linear elasticity. Int J Solids Struct 1965; 1: 417–438. https://doi.org/10. 1016/0 020-7683(65)90 0 06-5
51. Aifantis EC. On the role of gradients in the localization of deformation and fracture. Int J Eng Sci 1992; 3: 1279–1299. https://doi.org/10.1016/0020-7225(92)90141-3
52. Lam DCC, Yang F, Chong ACM, Wang J, Tong P. Experiments and theory in strain gradient elasticity. J Mech Phys Solids 2003; 51: 1477–1508. https://doi.org/10.1016/S0022-5096(03)00053-X

53. Aifantis EC. Update on a class of gradient theories. Mech Mater 2003; 35: 259–280. https://doi.org/10.1016/S0167-6636(02)00278-8

54. Aifantis EC. On the gradient approach–relation to Eringen's nonlocal theory. Int J Eng Sci 2011; 49: 1367–1377. https://doi.org/10.1016/j.ijengsci.2011.03.016

55. Lim CW, Zhang G, Reddy JN. A higher-order nonlocal elasticity and strain gradient theory and its applications in wave propagation. J Mech Phys Solids 2015; 78: 298–313. https://doi.org/10.1016/j.jmps.2015.02.001

56. Faghidian SA. Reissner stationary variational principle for nonlocal strain gradient theory of elasticity. Eur J Mech A Solids 2018; 70: 115-126. https://doi.org/10.1016/j.euromechsol.2018.02.009

57. Faghidian SA. On non-linear flexure of beams based on non-local elasticity theory. Int J Eng Sci 2018; 124: 49–63. https://doi.org/10.1016/j.ijengsci.2017.12.002

58. Faghidian SA. Integro-differential nonlocal theory of elasticity. Int J Eng Sci 2018; 129: 96–110. https://doi.org/10.1016/j.ijengsci.2018.04.007

59. Barretta R, Marotti de Sciarra F. Constitutive boundary conditions for nonlocal strain gradient elastic nano-beams. Int J Eng Sci 2018; 130: 187-198. https://doi.org/10.1016/j.ijengsci.2018.05.009

60. Apuzzo A, Barretta R, Faghidian SA, Luciano R, Marotti de Sciarra F. Free vibrations of elastic beams by modified nonlocal strain gradient theory. Int J Eng. Sci 2018; 133: 99–108. https://doi.org/10.1016/j.ijengsci.2018.09.002

61. Apuzzo A, Barretta R, Faghidian SA, Luciano R, Marotti de Sciarra F. Nonlocal strain gradient exact solutions for functionally graded inflected nano-beams. Compos Part B 2019; 164: 667-674. https://doi.org/10.1016/j.compositesb.2018.12.112

62. Barretta R, Čanadija M, Marotti de Sciarra F. Modified Nonlocal Strain Gradient Elasticity for Nano-Rods and Application to Carbon Nanotubes. Appl Sci 2019; 9: 514. https://doi.org/10.3390/app9030514

63. Demir Ç, Civalek Ö. Torsional and longitudinal frequency and wave response of microtubules based on the nonlocal continuum and nonlocal discrete models. Appl Math Modell 2013; 37: 9355–67. http://dx.doi.org/10.1016/j.apm.2013.04.050

64. Li C. Torsional vibration of carbon nanotubes: comparison of two nonlocal models and a semi-continuum model. Int J Mech Sci 2014; 82: 25–31. http://dx.doi.org/10.1016/j.ijmecsci.2014.02.023

65. Li C. A nonlocal analytical approach for torsion of cylindrical nanostructures and the existence of higher-order stress and geometric boundaries. Compos Struct 2014; 118: 607-621. https://doi.org/10.1016/j.compstruct.2014.08.008

66. Arda M, Aydogdu M. Torsional statics and dynamics of nanotubes embedded in an elastic medium. Compos Struct 2014; 114: 80-91. https://doi.org/10.1016/j.compstruct.2014.03.053.

67. Barretta R, Feo L, Luciano R. Torsion of functionally graded nonlocal viscoelastic circular nanobeams. Compos Part B 2015; 72: 217–222. http://dx.doi.org/10.1016/j.compositesb.2014.12.018

68. Marotti de Sciarra F, Čanađija M, Barretta R. A gradient model for torsion of nanobeams. CR Mec 2015; 343: 289-300. https://doi.org/10.1016/j.crme.2015.02.004

69. Apuzzo A, Barretta R, Čanađija M, Feo L, Luciano R, Marotti de Sciarra F. A closed-form model for torsion of nanobeams with an enhanced nonlocal formulation. Compos Part B 2017; 108: 315–324. https://doi.org/10.1016/j.compositesb.2016.09.012

70. Kahrobaiyan MH, Tajalli SA, Movahhedy MR, Akbari J, Ahmadian MT. Torsion of strain gradient bars. Int J Eng Sci 2011; 49: 856-866. https://doi.org/10.1016/j.ijengsci.2011.04.008

71. Polyzos D, Huber G, Mylonakis G, Triantafyllidis T, Papargyri-Beskou S, Beskos D. Torsional vibrations of a column of fine-grained material: a gradient elastic approach. J Mech Phys Solids 2015; 76: 338–358. http://dx.doi.org/10.1016/j.jmps.2014.11.012

72. Lazopoulos KA, Lazopoulos AK. On the torsion problem of strain gradient elastic bars. Mech. Res. Commun. 2014; 45: 42-47. https://doi.org/10.1016/j.mechrescom.2012.06.007.

73. Barretta R, Diaco M, Feo L, Luciano R, Marotti de Sciarra F, Penna R. Stress-driven integral elastic theory for torsion of nano-beams. Mech Res Commun 2018; 87: 35-41. https://doi.org/10.1016/j.mechrescom.2017.11.004

74. Barretta R, Faghidian SA, Luciano R, Medaglia CM, Penna R. Stress-driven two-phase integral elasticity for torsion of nano-beams. Compos Part B 2018; 145: 62-69. https://doi.org/10.1016/j.compositesb.2018.02.020

75. Zhu X, Li L. Twisting statics of functionally graded nanotubes using Eringen's nonlocal integral model. Compos Struct 2017; 178: 87–96. http://dx.doi.org/10.1016/j.compstruct.2017.06.067

76. Guo S, He Y, Liu D, Lei J, Shen L, Li Z. Torsional vibration of carbon nanotube with axial velocity and velocity gradient effect. Int J Mech Sci 2016; 119: 88–96. http://dx.doi.org/10.1016/j.ijmecsci.2016.09.036

77. Shen Y, Chen Y, Li L. Torsion of a functionally graded material. Int J Eng Sci 2016; 109: 14–28. http://dx.doi.org/10.1016/j.ijengsci.2016.09.003

Table 1. Normalized maximum torsional rotation of doubly clamped FG nano-beam: NLSG $\left(\ell_1 \neq 0\right)$ vs. MSNG

	$\frac{\bar{\varphi}_{\max}}{\bar{\varphi}_{\max}^{\mathrm{LOC}}}$									
	NLSG $\left(\ell_1 \neq 0\right)$					MNSG				
λ	$\mu_1 = 0.1$	$\mu_1 = 0.3$	$\mu_1 = 0.5$	$\mu_1 = 0.7$	$\mu_1 = 1.0$	$\mu_s = 0.1$	$\mu_s = 0.3$	$\mu_s = 0.5$	$\mu_s = 0.7$	$\mu_s = 1.0$
0^+	0.95743	0.69358	0.44286	0.28687	0.16403	0.92108	0.54261	0.29611	0.17604	0.094552
0.2	2.07504	1.58731	1.02786	0.668904	0.38347	2.02599	1.2541	0.690288	0.411456	0.221314
0.4	3.8313	2.99176	1.94714	1.26924	0.728309	3.76227	2.37216	1.30971	0.781398	0.420513
0.6	6.2262	4.90691	3.20071	2.08789	1.19854	6.12993	3.89679	2.15438	1.28586	0.692147
0.8	9.25973	7.33278	4.78856	3.12483	1.79417	9.12896	5.82798	3.2243	1.92486	1.03622
1.0	12.9319	10.2693	6.7107	4.38009	2.5152	12.7594	8.16574	4.51946	2.69837	1.45272

Table 2. Normalized maximum torsional rotation of doubly clamped FG nano-beam: NLSG $\left(\ell_2 \neq 0\right)$

	$\frac{\bar{\varphi}_{\max}}{\bar{\varphi}_{\max}^{\mathrm{LOC}}}$					
	NLSG $\left(\ell_2 \neq 0\right)$					
λ	$\mu_2 = 0.01$	$\mu_2 = 0.1$	$\mu_2 = 0.3$	$\mu_2 = 0.5$	$\mu_2 = 0.7$	$\mu_2 = 1.0$
0^+	0.94322	0.14245	0.018122	0.0066006	0.0033786	0.0016584
0.2	1.99982	0.302449	0.038486	0.014018	0.007175	0.003522
0.4	3.6602	0.553878	0.070486	0.025673	0.013141	0.00645
0.6	5.92435	0.896735	0.114122	0.041568	0.021277	0.010444
0.8	8.79227	1.33102	0.169395	0.0617	0.031582	0.015502
1.0	12.264	1.85673	0.236304	0.086071	0.044057	0.021625

Table 3. Normalized mid-span torsional rotation of cantilever FG nano-beam: NLSG$\left(\ell_1 \neq 0\right)$ vs. MSNG

	$\frac{\overline{\varphi}_{x=1/2}}{\overline{\varphi}^{\mathrm{LOC}}_{x=1/2}}$									
	NLSG$\left(\ell_1 \neq 0\right)$					MNSG				
λ	$\mu_1 = 0.1$	$\mu_1 = 0.3$	$\mu_1 = 0.5$	$\mu_1 = 0.7$	$\mu_1 = 1.0$	$\mu_s = 0.1$	$\mu_s = 0.3$	$\mu_s = 0.5$	$\mu_s = 0.7$	$\mu_s = 1.0$
0^+	0.98581	0.89786	0.81429	0.76229	0.72134	0.97370	0.84754	0.76537	0.72535	0.69819
0.2	1.62501	1.46244	1.27595	1.1563	1.06116	1.60866	1.35137	1.16343	1.07049	1.0071
0.4	2.4771	2.19725	1.84905	1.62308	1.44277	2.45409	1.99072	1.63657	1.46047	1.34017
0.6	3.54207	3.1023	2.53357	2.16263	1.86618	3.50998	2.7656	2.18479	1.89529	1.69738
0.8	4.81991	4.17759	3.32952	2.77494	2.33139	4.77632	3.67599	2.8081	2.37495	2.07874
1.0	6.31064	5.42312	4.2369	3.46003	2.8384	6.25312	4.72191	3.50649	2.89946	2.48424

Table 4. Normalized mid-span torsional rotation of cantilever FG nano-beam: NLSG $\left(\ell_2 \neq 0\right)$

	$\frac{\overline{\varphi}_{x=1/2}}{\overline{\varphi}_{x=1/2}^{\mathrm{LOC}}}$					
	NLSG$\left(\ell_2 \neq 0\right)$					
λ	$\mu_2 = 0.01$	$\mu_2 = 0.1$	$\mu_2 = 0.3$	$\mu_2 = 0.5$	$\mu_2 = 0.7$	$\mu_2 = 1.0$
0^+	0.94334	0.14272	0.018162	0.0066152	0.0033861	0.0016621
0.2	1.54711	0.23415	0.029798	0.010854	0.005556	0.002727
0.4	2.35214	0.356054	0.045314	0.016505	0.008448	0.004147
0.6	3.35843	0.508435	0.064707	0.023569	0.012064	0.005922
0.8	4.56598	0.691293	0.08798	0.032046	0.016403	0.008051
1.0	5.97478	0.904626	0.115132	0.041935	0.021465	0.010536

Table 5. Normalized torsional fundamental frequencies of doubly clamped FG nano-beam: NLSG$\left(\ell_1 \neq 0\right)$ vs. MSNG

	$\frac{\bar{\omega}}{\bar{\omega}_{\mathrm{LOC}}}$									
	NLSG$\left(\ell_1 \neq 0\right)$					MNSG				
λ	$\mu_1 = 0.1$	$\mu_1 = 0.3$	$\mu_1 = 0.5$	$\mu_1 = 0.7$	$\mu_1 = 1.0$	$\mu_s = 0.1$	$\mu_s = 0.3$	$\mu_s = 0.5$	$\mu_s = 0.7$	$\mu_s = 1.0$
0^+	1.02393	1.21155	1.51878	1.88811	2.49775	1.04609	1.37139	1.85837	2.41097	3.29032
0.2	0.686622	0.817239	1.02552	1.27531	1.68738	0.702992	0.92573	1.2552	1.62873	2.22298
0.4	0.496445	0.591996	0.743019	0.924042	1.22265	0.508701	0.670681	0.909472	1.18015	1.61076
0.6	0.385248	0.459185	0.576228	0.716575	0.948107	0.394737	0.520155	0.705278	0.915153	1.24905
0.8	0.313716	0.373568	0.468695	0.582814	0.771099	0.321349	0.42311	0.573627	0.7443	1.01584
1.0	0.264189	0.314298	0.394267	0.490239	0.648599	0.27053	0.355938	0.482513	0.626059	0.854447

Table 6. Normalized torsional fundamental frequencies of doubly clamped FG nano-beam:

$\mathrm{NLSG}\left(\ell_2 \neq 0\right)$

$\frac{\bar{\omega}}{\bar{\omega}_{\mathrm{LOC}}}$						
	$\mathrm{NLSG}\left(\ell_2 \neq 0\right)$					
λ	$\mu_2 = 0.01$	$\mu_2 = 0.1$	$\mu_2 = 0.3$	$\mu_2 = 0.5$	$\mu_2 = 0.7$	$\mu_2 = 1.0$
0^+	1.02762	2.64511	7.41629	12.2886	17.1763	24.5164
0.2	0.681796	1.76013	4.93627	8.1795	11.4329	16.3186
0.4	0.490241	1.26775	3.55592	5.8923	8.23596	11.7556
0.6	0.379948	0.983072	2.75753	4.56935	6.38682	9.11623
0.8	0.309473	0.800805	2.24628	3.72219	5.2027	7.42606
1.0	0.260812	0.67484	1.89292	3.13666	4.38427	6.25788

Table 7. Normalized torsional fundamental frequencies of cantilever FG nano-beam: NLSG $(\ell_1 \neq 0)$ vs. MSNG

	$\frac{\bar{\omega}}{\bar{\omega}_{\mathrm{LOC}}}$									
	NLSG $(\ell_1 \neq 0)$					MNSG				
λ	$\mu_1 = 0.1$	$\mu_1 = 0.3$	$\mu_1 = 0.5$	$\mu_1 = 0.7$	$\mu_1 = 1.0$	$\mu_s = 0.1$	$\mu_s = 0.3$	$\mu_s = 0.5$	$\mu_s = 0.7$	$\mu_s = 1.0$
0^+	1.0046	1.0324	1.05739	1.07297	1.08529	1.00881	1.04746	1.07204	1.08408	1.09229
0.2	0.819725	0.858452	0.895339	0.919611	0.939497	0.825677	0.880371	0.91814	0.93752	0.951042
0.4	0.676587	0.724273	0.771502	0.804129	0.831834	0.68401	0.752015	0.802117	0.829042	0.848321
0.6	0.570779	0.621903	0.675341	0.714186	0.748477	0.57862	0.652907	0.711743	0.744967	0.769457
0.8	0.491435	0.542649	0.599054	0.642062	0.681525	0.499123	0.575002	0.639306	0.677421	0.706371
1.0	0.430438	0.480102	0.537358	0.582915	0.626286	0.437734	0.512614	0.579944	0.621704	0.654384

Table 8. Normalized torsional fundamental frequencies of cantilever FG nano-beam: NLSG $\left(\ell_2 \neq 0\right)$

$\frac{\bar{\omega}}{\bar{\omega}_{\mathrm{LOC}}}$						
	NLSG $\left(\ell_2 \neq 0\right)$					
λ	$\mu_2 = 0.01$	$\mu_2 = 0.1$	$\mu_2 = 0.3$	$\mu_2 = 0.5$	$\mu_2 = 0.7$	$\mu_2 = 1.0$
0^+	1.02856	2.64423	7.41237	12.2819	17.1668	24.5028
0.2	0.833317	2.14541	6.01489	9.9665	13.9305	19.8836
0.4	0.681752	1.75839	4.93068	8.17012	11.4197	16.2998
0.6	0.571601	1.4761	4.13962	6.8594	9.58769	13.6849
0.8	0.490219	1.2669	3.55318	5.88771	8.22953	11.7464
1.0	0.42833	1.10746	3.10614	5.14697	7.19416	10.2686